Short-term wind speed prediction based on FEEMD-PE-SSA-BP

Ting Zhu (zhuting20210422@163.com)
Wuhan University of Science and Technology
wenbo wang
Wuhan University of Science and Technology
MIN YU
Wuhan University of Science and Technology

Research Article

Keywords: wind speed prediction, sparrow search algorithm, permutation entropy, BP neural network, FEEMD

Posted Date: March 29th, 2022

DOI: https://doi.org/10.21203/rs.3.rs-1425821/v1

Short-term wind speed prediction based on FEEMD-PE-SSA-BP

Ting Zhu, Wenbo Wang &Min Yu

School of Science, Wuhan University of Science and Technology, Wuhan 430081, China

Abstract: As one of the renewable energy power generation methods, wind power generation shows a high growth trend. However, while wind power is connected to the grid,the volatility and instability of wind power make the power system produce a lot of uncertain fluctuations , which greatly affects the power quality and jeopardizes the stable operation of the power system. Therefore, high wind speed forecasting accuracy can provide a solid basis for grid management,, improve the power system's ability to consume wind power, and ensure the safety and stabilization of the power system. In order to solve the problem of inaccurate prediction caused by the non-linearity and unsteadiness of wind speed series, this paper proposes a Fractal Ensemble Empirical Mode Decomposition (FEEMD)-Permutation Entropy (PE)-Sparrow Search Algorithm (SSA)-Error Back Propagation (BP) neural network method for short-term wind speed prediction. This method first uses the fractal dimension-based ensemble empirical modal decomposition (FEEMD) to decompose the original wind speed in order from high to low frequency; then calculates the entropy value of each component, and merges the components with similar entropy values to effectively reduce the computation; finally, the new sub-series are predicted by SSA-BP model, and the predicted value of the merged new sub-sequence is accumulated to obtain the final wind speed prediction result. The simulation study shows that the proposed prediction model is not only fast and accurate, but also suitable for short-term wind speed prediction.

Keywords: wind speed prediction; sparrow search algorithm; permutation entropy; BP neural network; FEEMD

1 Introduction

With the rapid development of China's economy, the consumption of fossil fuels has also increased sharply, which has also brought many environmental problems. As one of the most potential renewable energy sources, various countries are paying close attention to its development and utilization. However, when we use wind energy for power generation, due to the influence of factors such as temperature, terrain, latitude, etc., the wind speed will show strong volatility and non-linearity, which will increase the uncertainty of wind power generation(Bo Ming 2019). This uncertainty will have a huge impact on the power quality , and even threaten the stabilization and safety of power grid system. In order to minimize the impact of wind speed volatility and non-linearity, accurate wind speed prediction is essential for energy suppliers and grid operators. Wind speed forecasts will not only benefit energy suppliers, but will also try to balance the growing global demand for electricity. Therefore, accurate wind speed prediction has made an essential contribution to power generation management and control system (Cui Yanbin 2019).Wind speed forecasting can be classified by time duration: ultra-short-term forecasting (less

than 0.5 h), short-term forecasting (0.5-72 h), and medium- and long-term forecasting (greater than 72 h). Classified by method, there are a number of methods which mainly include (1)physical models(Gupta,D 2021); (2)conventional statistical models such as auto-regressive (AR) models, auto-regressive moving average models (ARMA) and auto-regressive integrated moving average (ARIMA) models (Aasim,S.N 2019; Wenlong Fu et al. 2019);(3)artificial intelligence methods, such as neural networks, Extreme Learning Machine (ELM),long and short-term memory network (LSTM)and BP neural network method(BP)(Jaseena K.U. 2021; Chen Gonggui et al. 2022 and K U Jaseena 2021);(4) combined forecasting and mixed forecasting(Li Dan 2022; Zhang Shuai et al. 2021; Liao Xuechao 2021 and Shouxiang Wang 2016), etc. Among them, BP neural network is the most widely used, but the disadvantage is that the convergence speed is slow and easy to fall into the local optimum, currently most optimization algorithms are used to find the optimal weights and thresholds of BP neural network(Yanfei Li 2018). In addition, it was shown that for the prediction of wind speed series the decomposition method can effectively reduce the non-smoothness of wind speed(Hui Liu 2018; Huanling Hu et al. 2021). Common decomposition methods include empirical modal decomposition (EMD), empirical ensemble modal decomposition (EEMD), and complementary ensemble empirical modal decomposition (CEEMD). EMD(Huang Norden E 1998)is an adaptive signal time-frequency decomposition method. Compared with wavelet decomposition, it solves the problem of non-adaptive basis function, but it will cause more serious modal aliasing in the decomposition process. EEMD(Wu Z H 2009) suppresses modal aliasing to a certain extent by adding white noise to the signal, but there is a certain degree of damage to the original signal, and the added white noise will affect reconstruction error if the amplitude is not appropriate. In addition, in the process of selecting components for EEMD, the upper envelope and lower envelope will diverge at both ends of the data sequence, which is called the end effect. End effect will increase some false components, therefore, effective end effect suppression at both ends of the signal is of great significance. Han Jianping et al.(2010) have proposed mirror continuation, parallel continuation(He Zhenpeng 2018), double symmetric continuation(Xiang Hong 2016), polynomial fitting(Liu Huiting 2004)and other methods for this problem, which can restrain the phenomenon of boundary divergence to a certain extent. CEEMD(Yeh J R 2010)adds a positive and negative white noise to original signal to neutralize the impact on the original signal, but it increases the amount of calculation and is prone to false components. Zheng Jinde(2014) proposed a modified ensemble empirical mode decomposition (MEEMD), which first uses CEEMD to decompose the original sequence in order of frequency, and then according to the entropy value of the permutation of the components, the abnormal components are distinguished and removed from the original signal. Finally, EMD is performed on the signal after removing the abnormal signal. This method can effectively suppress the modal aliasing phenomenon of EMD and overcome the problem of improper noise amplitude in EEMD. A key step in the MEEMD method is about the detection of high frequency or intermittent signals, however, there are many detection methods, such as the detection of smoothness and non-smoothness proposed by Xiao(2007) and others, the detection of noise energy proposed by Terrien(2011) and others, and the detection of signal randomness based on alignment entropy proposed by Zheng Jinde (2013). Inspired by the above ideas, this paper introduces a new detection method--signal randomness detection based on fractal dimension, and subsequently proposes a new decomposition method-- Ensemble Empirical Mode Decomposition based on fractal dimension(FEEMD), and applies this new decomposition method to short-term

wind speed prediction.

In this paper, the FEEMD decomposition method is used to decompose the original wind speed series into a series of relatively stable IMF series, and the ranking entropy is used to measure the complexity of each IMF, and then the components with close entropy values are combined to obtain new components to reduce the amount of operations, and then the SSA-BP neural network is built for each new component. Last but not least, the prediction results of each new sub-series are accumulated to gather the final wind speed prediction. This paper shows that the accuracy of the wind speed prediction model has been effectively improved through the experimental simulation of the actual wind speed collected from Canada and Hawaii.

The organization structure of this paper is as follows: The second section introduces the box-counting dimension in fractal dimension, the construction of FEEMD algorithm and the analysis of FEEMD algorithm decomposition performance. In section 3, the FEEMD-PE algorithm is proposed. The fourth section introduces the establishment process of BP neural network, sparrow search algorithm and FEEMD-PE-SSA-BP wind speed prediction model. Part V of this paper presents the prediction results of the FEEMD-PE-SSA-BP model for two wind farms in Canada and Hawaii and a comparison with the prediction results of other models. The last part of this paper provides conclusions for this research and develops the next research plan.

2 FEEMD algorithm

EEMD and CEEMD make the distribution of the polar points of the original signal more uniform by adding white noise, and cover the abnormal signals such as high-frequency intervals or noise in the original signal, so that the confusion of modes can be attenuated or even eliminated by decomposing with EMD. However, due to the limitation of the number of iterations, the components obtained from the decomposition may not satisfy the definition of IMF(Fuzheng Liu, 2020). Therefore, the obtained components may not be IMF in the strict sense.It makes no sense from the application point of view to sacrifice the accuracy of the components for the adaptive nature of the decomposition, as well as the inability to guarantee that the instantaneous frequency of the components has physical significance. And it is the purpose of this paper to guarantee the adaptability of the decomposition on the basis of ensuring that the components have physical meaning.

As a matter of fact, when the abnormal signal is decomposed, it’s not required to perform the complete EMD of the added noise, but just to ensure the completeness of the decomposition of the added noise signal. Based on this, the paper improves the EEMD and CEEMD methods and proposes an overall average empirical mode decomposition based on the fractal dimension(FEEMD) .

2.1 Introduction to Fractal Dimension

The fractal dimension is an important parameter that can describe the singularity degree of chaotic attractors, which reflects the fundamental characteristics of the system fractals and is often used to study the characteristics of the behavior of nonlinear systems and wind power prediction. Fractal dimensions can be broadly categorized as Hausdorff dimensions, associative dimensions, box counting dimensions, and lattice dimensions(Renato Huzak 2021), which depends on the calculation methods and principles. The correlation dimension can reflect the in-homogeneity of attractors of nonlinear systems more sensitively, especially the dynamic structure of attractors, and

can better describe the dimensional and chaotic properties of complex systems. Box-counting dimension is not only a measurement parameter to describe the irregularity of complex shapes, but also a method to detect the randomness and dynamic changes of time series. It is often used in time series analysis and image processing. Hausdorff dimension is the basis of fractal geometry. Because its mathematical definition is very strict, it is often used in some theoretical derivations of fractal geometry. Since the box-counting method is simple and easy to operate ; this article will use the box-counting dimension to detect abnormal signals in wind speed.

2.2 Definition of counting box dimension

The principle of calculating the box dimension for wind speed time series is that a small square box with side length ε is taken to cover the waveform graph of the wind speed series to be processed. Some of the small boxes covered are empty because of the various layers of cavities and gaps inside the fractal. Mark the empty boxes as 0 and the non-empty boxes as 1, and count the number of boxes with 1 as $N(\varepsilon)$, this gives a set of $(\varepsilon, N(\varepsilon))$, then decrease the size of the small box ε, the number of non-empty small boxes $N(\varepsilon)$ obtained will necessarily increase, this will give a series of $(\varepsilon, N(\varepsilon))$, taking the logarithm of ε and $N(\varepsilon)$ respectively, and then fitting a straight line with $\ln\varepsilon$ as the horizontal coordinate and $\ln N(\varepsilon)$ as the vertical coordinate to find the slope of $\ln N(\varepsilon)$ to $\ln\varepsilon$ .The negative value of its slope is the box counting dimension of the wind speed series waveform graph, which is calculated as follows：

$$D = -\lim_{\varepsilon \to 0} \frac{\ln N(\varepsilon)}{\ln \varepsilon} \tag{1}$$

The box can better approximate the fractal body. However, after the scale is further reduced to a certain point, the limit of resolution is reached. Therefore, the box size should not be infinitely small, but not too small. In this paper, the number of boxes $N(\varepsilon)$ is chosen to be 2^{20} .

2.3 Construction of FEEMD algorithm

Based on the randomness detection of counting box dimension, FEEMD algorithm is first proposed to decompose raw wind speed signal in the paper. The essence of FEEMD is to decompose the original signal in order of frequency by CEEMD method, then calculate the counting box dimension value of each component, compare the counting box dimension of each component with the threshold value of counting box dimension set, then the abnormal signal can be detected and separated from the original signal, and then implement EMD decomposition for the remaining signal. For a set of non-stationary signals $S(t)$, the FEEMD method decomposition steps are as follows.

(1) In the original signal $S(t)$, add paired white noise signals $n_i(t)$ and -$n_i(t)$ with a mean value of 0 respectively, thereby constructing two new signals $s_i^+(t)$ and $s_i^-(t)$. which is:

$$S_i^+(t) = S(t) + a_i n_i(t) \tag{2}$$

$$S_i^-(t) = S(t) - a_i n_i(t) \tag{3}$$

Among them: a_i represents the amplitude of the added white noise signal, $i = 1, 2, \mathrm{L}\ , Ne$, Ne means the logarithm of the added white noise, and Ne is generally within 100. Perform EMD on $S_i^+(t)$ and $S_i^-(t)$ respectively, and get the first-order IMF component sequences $\left\{I_{i1}^+(t)\right\}$ and $\left\{I_{i1}^-(t)\right\}$ $(i = 1, 2, \mathrm{L}\ , Ne)$. Integrate and average the above-obtained components:

$$I_1(t) = \frac{1}{2N} \sum_{i=1}^{Ne} \left[I_{i1}^+(t) + I_{i1}^-(t) \right] \tag{4}$$

Check whether $I_1(t)$ is an abnormal signal: If the box-counting dimension of the signal is greater than θ_0 , it will be regarded as an abnormal signal**Error! Reference source not found.**, otherwise it is approximately regarded as a stationary signal. After many simulation experiments, it is found

that 1.22~1.24 is more appropriate for θ_0 , and 1.22 is used in this article.

(2) If $I_1(t)$ is an anomalous signal, then we continue to perform step (1) until the IMF component $I_P(t)$ is a normal signal.

(3) Separate the previous decomposed component from the original signal, namely:

$$r(t) = S(t) - \sum_{j=1}^{p-1} I_j(t) \tag{5}$$

(4) EMD is used to decompose the remaining signal $r(t)$ after the abnormal signal is separated to obtain IMFs and Rs, that is, FEEMD is completed.

2.4 Decomposition performance analysis of FEEMD algorithm

In order to verify the effectiveness of FEEMD method in this paper, without loss of generality, examine the simulated signal:

$$s(t) = 2\sin(60\pi t + \pi/2) + (t+1)\sin(16\pi t + \pi/3) + n(t) \tag{6}$$

Among them: $t = 1/4096 : 1/4096 : 1$, $n(t)$ is Gaussian white noise signal of 20db, the simulation signal is decomposed by EMD, CEEMD, MEEMD, FEEMD, as shown in Figure 1-4. There are 9 EMD components, and the first 5 are shown in Figure 1. There are 12 CEEMD components in total, and the first 6 are shown in Figure 2. MEEMD decomposes a total of 5 IMFs and 1 RS in Figure 3, while FEEMD decomposes a total of 1 IMF and 1 RS in Figure 4.

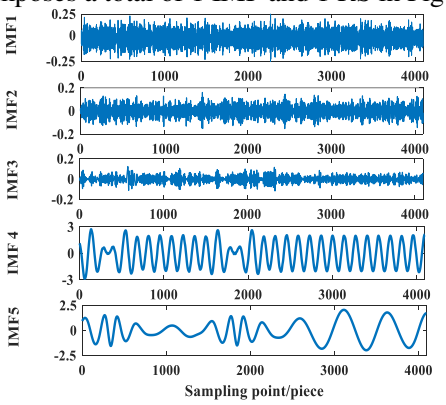

Fig.1 EMD effects of simulation signal

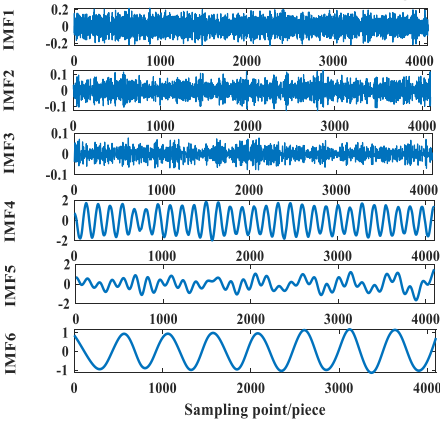

Fig.2 CEEMD effects of simulation signal

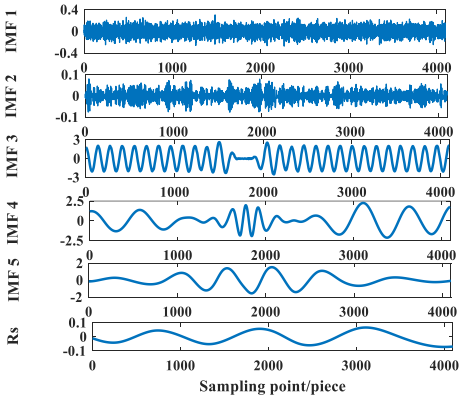

Fig.3 MEEMD effects of simulation signal

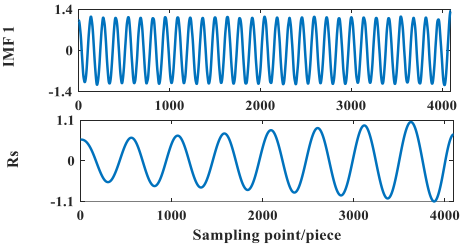

Fig.4 FEEMD effects of simulation signal

It can be seen from the decomposition of Figure 1-4: Compared with the other three methods, the FEEMD decomposes the high-frequency components more thoroughly, smoothing the data better. The high-frequency component waveform is extremely symmetrical up and down, with obvious periodicity.

3 FEEMD-PE algorithm

Aiming at the problem of decomposing some IMF components of similar complexity in the FEEMD method, this paper introduces the concept of Permutation Entropy (PE) to quantify the complexity of each IMF component, and then merge the IMF components of similar complexity to reduce IMF component. Permutation entropy is an index to measure the randomness of time series, which has the advantages of simple principle, fast calculation, and strong robustness(Qin Zhou 2020)0. Compared with the problem that the sample entropy is greatly affected by the length of the time series and the embedding dimension, the permutation entropy is not affected by the length of time series, which makes up for this defect.

Let the time series(Liang Tao 2021) be $\{X(i), i=1,2,\mathrm{L}\ ,n\}$. Reconstruct the phase space of the time series to get the matrix(Tian X 2019):

$$\begin{bmatrix} x(1) & x(1+\tau) & \mathrm{L} & x[1+(m-1)\tau \\ \mathrm{M} & \mathrm{M} & & \mathrm{M} \\ x(j) & x(j+\tau) & \mathrm{L} & x[j+(m-1)\tau \\ \mathrm{M} & \mathrm{M} & & \mathrm{M} \\ x(K) & x(K+\tau) & \mathrm{L} & x[K+(m-1)\tau \end{bmatrix} \tag{7}$$

Where: $j=1,2,\mathrm{L}\ ,K$; m,τ are the embedding dimension and delay time. According to the numerical value, rearrange each reconstructed component in ascending order, where $j_1, j_2,\mathrm{L}\ , j_m$ is the column where each element in the reconstructed component is located. If the two elements of the reconstructed component have the same value, the order is defined according to the size of column j_1, j_2 where the elements are located. Therefore, for the matrix obtained after reconstruction of the phase space of the time sequence $X(i)$, each row obtains a set of symbol sequences.

$$S(l)=\left(j_1, j_2,\mathrm{L}\ , j_m\right) \tag{8}$$

Where: $l = 1,2,\mathrm{L}\ ,K,$ and $K = m!$, m-dimensional space can map $m!$ kinds of symbol sequences $(j_1, j_2,\mathrm{L}\ , j_m)$; $S(l)$ is a sequence of symbols, which is one of these permutations. If the occurrence probability of each symbol sequence is $p_1, p_2,\mathrm{L}\ , p_k$, then the permutation entropy of the time sequence $X(i)$ can be defined as:

$$H_P(m) = -\sum_{j=1}^{K} P_j \ln P_j \tag{9}$$

The permutation entropy reflects the randomness of the time series $X(i)$. The smaller the permutation entropy is, the more regular the time series are; on the contrary, the more random the time series are. The permutation entropy is used to quantify the complexity of IMF components and provide a basis for modal merging.

The principle of modal merging is: the closer the sample entropy of the component sequence is, the more similar the complexity is. Combining IMFs with similar complexity on the one hand can reduce the amount of modeling calculations and shorten the time used for modeling, on the other hand, it will not cause the original data to lose its essential characteristics.

4 FEEMD-PE-SSA-BP prediction model

This chapter is divided into the following two subsections. The first subsection introduces the structure of the SSA-BP neural network, and the second subsection introduces the algorithm steps of wind speed prediction model based on FEEMD-PE-SSA-BP.

4.1 The structure of SSA-BP neural network

In this section, the BP neural network and the sparrow search optimization algorithm are introduced respectively.

4.1.1 BP neural network

BP neural network has good self-organizing learning ability, it can realize any non-linear mapping from input to output. The principle is a multi-layer feed-forward network trained according to the error back propagation algorithm. In the propagation process, only one hidden layer can realize any n-dimension to m-dimension mapping. Figure 5 shows the model structure.

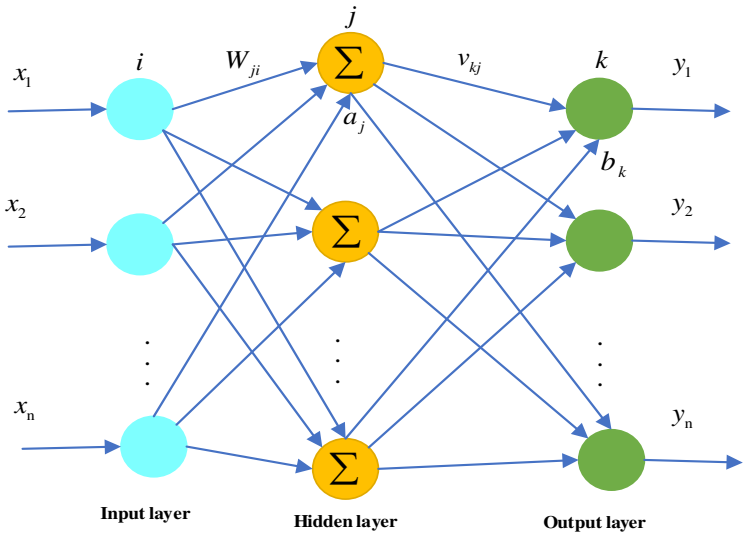

Fig.5 BP neural network model

The input value is x and the output value is y. j represents the weight between the i-th input layer and the j-th hidden layer, k represents the weight between the j-th hidden layer and the k-th output layer. a_j represents the threshold of the j-th neuron. b_k represents the threshold of the k-th neuron.

4.1.2 Sparrow Search Optimization Algorithm (SSA)

In the process of training, the most critical parameters for establishing the BP neural network model are the weight and threshold, and it is easy to fall into the local optimum when looking for the two. Jiankai Xue(2020)0proposed the Sparrow Search Algorithm (SSA) in 2020, which has good global optimization capabilities, so this paper uses it to optimize the weights and thresholds.

In nature, as a social bird, sparrows are smart and have strong memory. There is an obvious division of labor within the population(Zhou Shenghang 2020). Some sparrows are responsible for finding food and provide foraging areas and directions for the entire population, while the remaining sparrows use the former to obtain food. At the same time, when a sparrow is aware of the danger, it will issue an alarm signal in time, and the entire population will immediately make an anti-predation behavior.

In SSA, each sparrow position corresponds to a solution. There are three behaviors of sparrows in foraging: ①as a discoverer to find food; ②as a joiner to follow the discoverer for food; ③as a scout to decide whether the population gives up food. Among them, discoverers and joiners can be converted to each other, but the ratio remains constant, and discoverers account for 10% to 20% of the population. As the guide of foraging, the discoverer has a wide search range, and constantly updates his position through memory to obtain food sources. The joiner follows the discoverer to continue foraging to obtain a higher degree of fitness. However, due to the threat of predators at any time, the population will randomly select 10%-20% of sparrows as scouts for surveillance, so as to promptly remind the entire population to take anti-predation behavior when predators appear. The finder location is updated as follows:

$$x_{ij}^{t+1} = \begin{cases} x_{ij}^{t} \cdot \exp(\dfrac{-i}{\alpha \cdot MaxCycle}), R_2 < ST \\ x_{ij}^{t} + Q \cdot L, R_2 \geq ST \end{cases} \tag{10}$$

Where: $MaxCycle$ represents the maximum number of iterations of the algorithm;

$$x_{ij}^{t+1} = \begin{cases} Q \cdot \exp(\dfrac{x_{wj}^{t} - x_{ij}^{t}}{i^2}), i > NP/2 \\ x_{pj}^{t+1} + \left| x_{ij}^{t} - x_{pj}^{t+1} \right| \cdot A^{+} \cdot L, otherwise \end{cases} \tag{11}$$

In the formula, x_{pj}^{t} represents the best position of the discoverer in the $(t+1)$-th iteration， x_{wj}^{t} represents the global worst position at the t-th iteration; A represents a $1 \times d$ matrix, each element is randomly assigned a value of 1 or -1, and $A^{+} = A^{T} \cdot (AA^{T})^{-1}$. The location of the scout is updated as follows,

$$x_{ij}^{t+1} = \begin{cases} x_{ij}^{t} + \beta \cdot \left| x_{ij}^{t} - x_{bj}^{t} \right|, f_i \neq f_g \\ x_{ij}^{t} + K \dfrac{\left| x_{ij}^{t} - x_{wj}^{t} \right|}{(f_i - f_w) + \varepsilon}, f_i = f_g \end{cases} \tag{12}$$

In the formula, x_{bj}^{t} refers to the global best position in the t-th iteration， β, as the step length control parameter, is a normally distributed random number with a mean value of 0 and a variance of 1; K is a random number of $[-1,1]$; f_i, f_g, and f_w refer to the current fitness, global optimal, and worst fitness of the sparrow, respectively.

The SSA-BP model process is shown in Figure 6. The parameters of the sparrow search algorithm in this article are set as follows: the number of discoverers accounts for 20% of the entire population, the number of sparrows aware of danger SD accounts for 10%, and the safety threshold $ST = 0.8$. BP neural networks all use a 2-5-1 structure, and the output layer function uses the "traingdx" function.

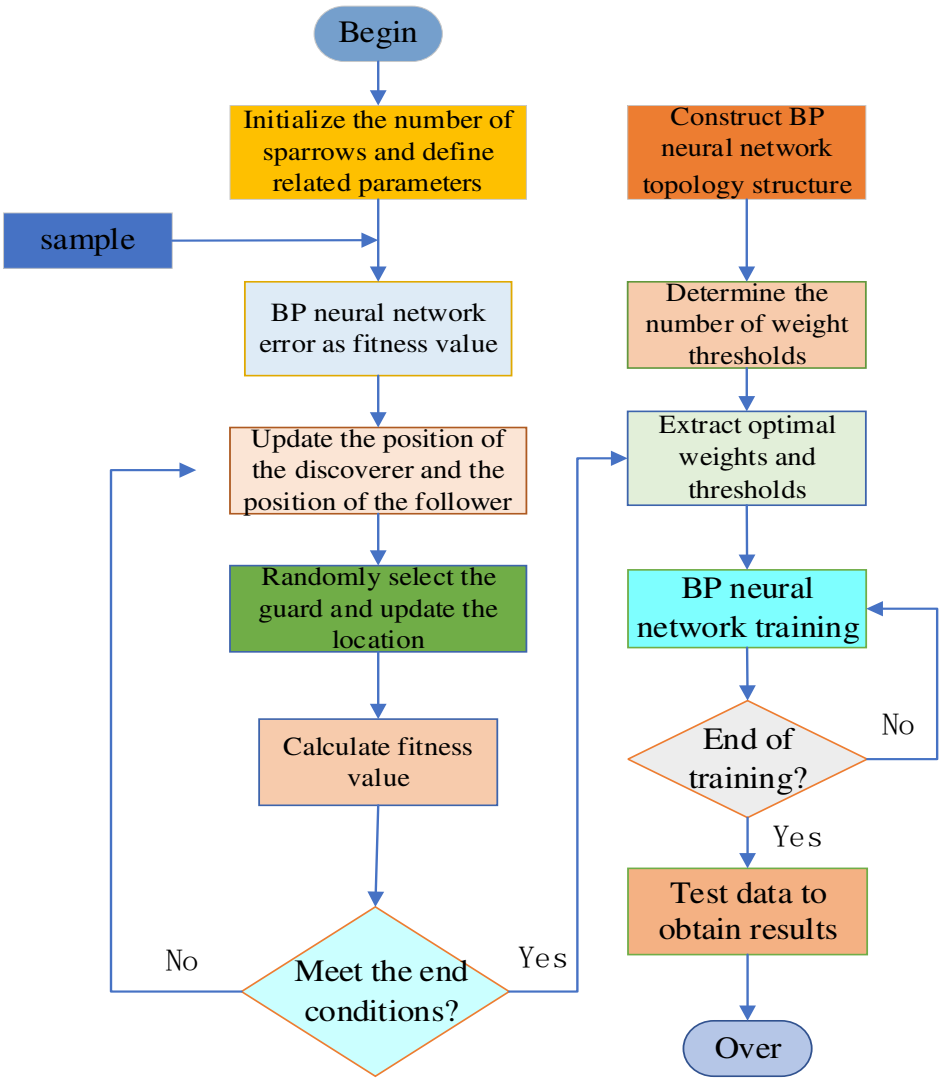

Fig.6 SSA-BP flow chart

4.2 Wind speed prediction model based on FEEMD-PE-SSA-BP

The steps of FEEMD-PE-SSA-BP algorithm are as follows:

1) Use the FEEMD method to decompose the original wind speed time series to obtain IMFs and Rs.

2) Calculate the permutation entropy value of IMFs, merge the sequences with close entropy values, and obtain the merged new component NIMFs.

3) Establish SSA-BP prediction model for each new component NIMFs, and get the predicted wind speed value of NIMFs.

4) The predicted value of NIMFs is superimposed to obtain the final predicted value. The FEEMD-PE-SSA-BP model process is shown in Figure 7.

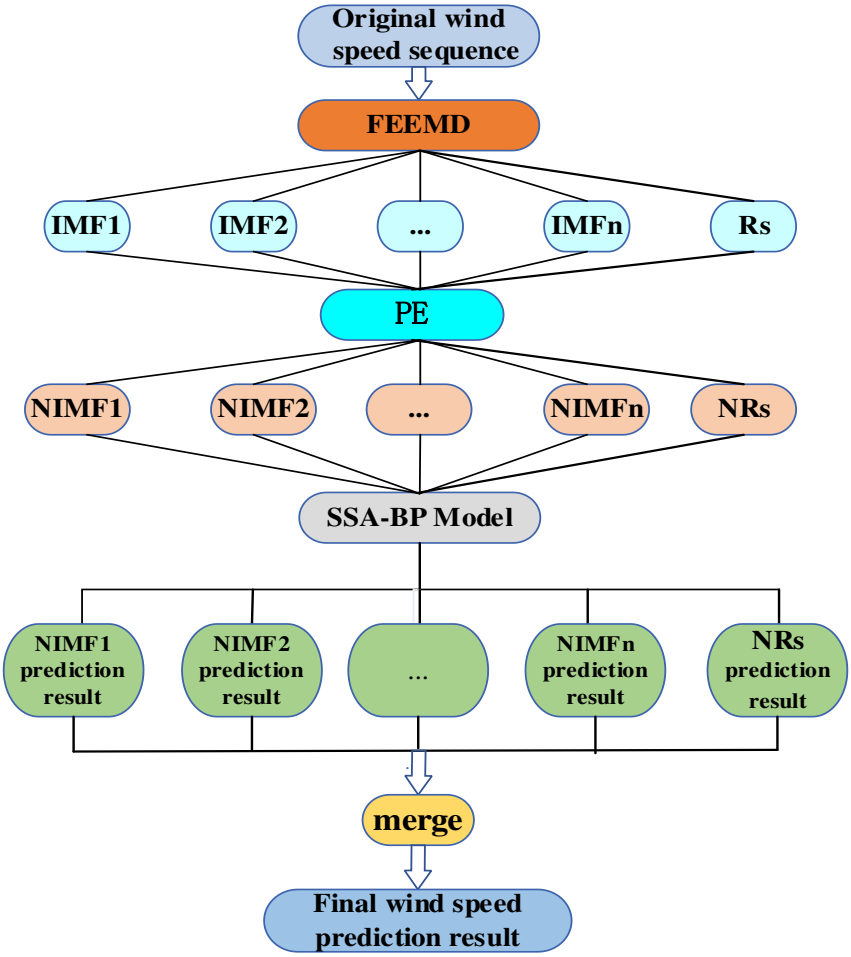

Fig.7 Flow chart of wind speed predition based on FEEMD-PE-SSA-BP

5 Experimental analysis

5.1 Experimental data

In order to verify the practicability about the method proposed in this paper, two sets of measured wind speed signals are investigated. One set of data from a wind farm in Abbotsford, Canada for 3 consecutive days from February 5th to 7th, and another set of data from a wind farm in Hawaii for 3 consecutive days from May 19th to 21st. The sampling time interval of the two sets of measured wind speed is 5 min, and each group has 864 data points. The first 701 groups are used as the experimental samples in the text, where the first 602 are used as the training set, and the remaining are the test set. The platform of this experiment is based on Matlab 2018a. The original time series of two wind farms are shown in Figure 8 and 9.

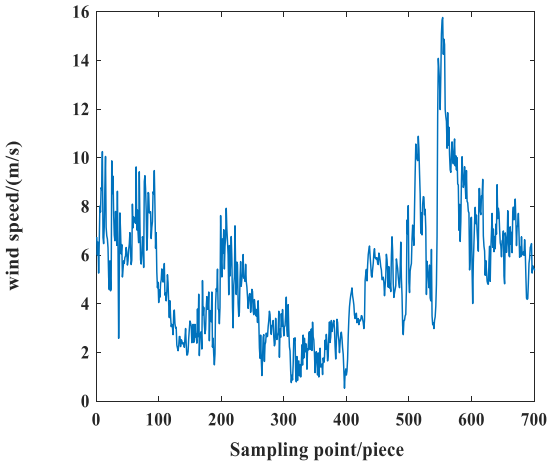

Fig.8 Original sequence of wind speed in Canada

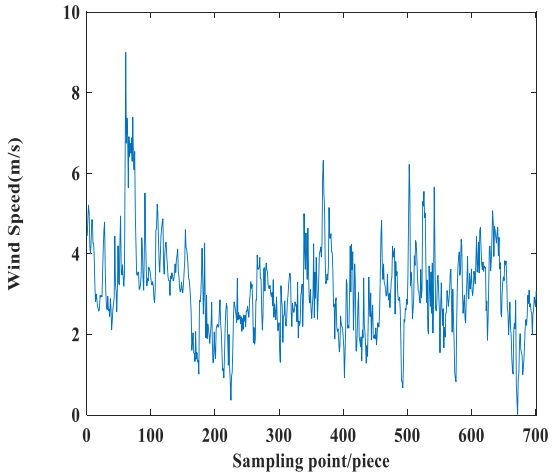

Fig.9 Original sequence of wind speed in Hawaii

5.2 Modal decomposition and evaluation of wind speed data

In order to demonstrate the effectiveness of FEEMD method, this paper compares it with EMD, EEMD, CEEMD, and MEEMD. Figures 10-14 merely show the decomposition results of EMD, EEMD, CEEMD, MEEMD, and FEEMD in Canada, respectively.These five decomposition methods all add white noise with I=50 group and standard deviation $\delta = 0.2$ .In addition, the embedding dimension of the MEEMD method $m = 6$ .The threshold of permutation entropy is $\theta = 0.6$ .The number of boxes in FEEMD is $N(\varepsilon) = 2^{20}$ .The box-counting dimension threshold is $\theta_0 = 1.22$.

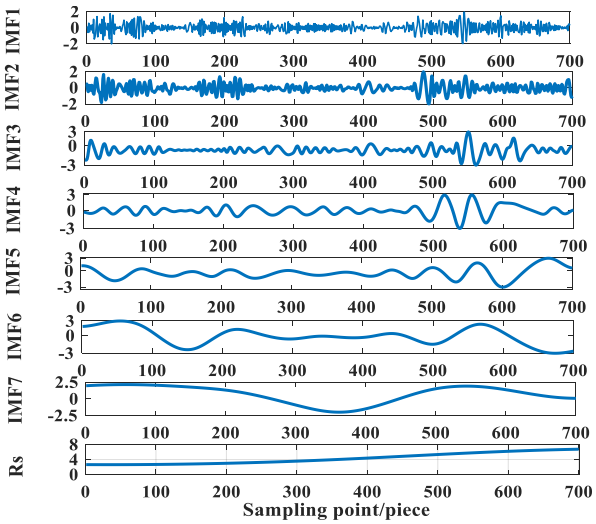

Fig.10 EMD effects of wind speed in Canada

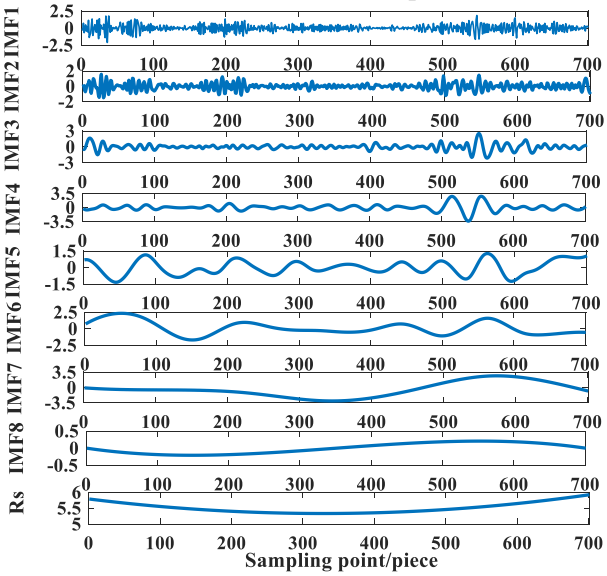

Fig.11 EEMD effects of wind speed in Canada

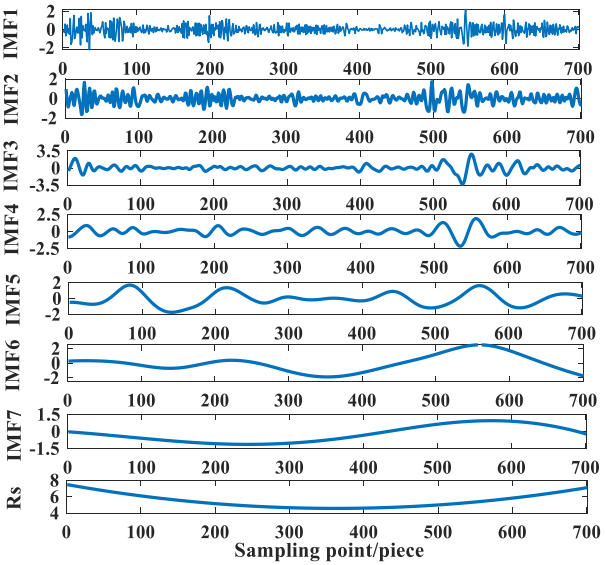

Fig.12 CEEMD effects of wind speed in Canada

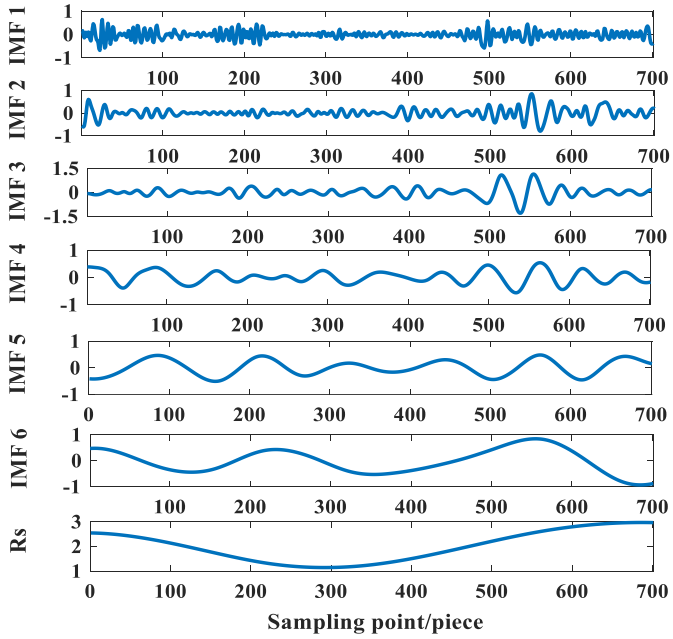

Fig.13 MEEMD effects of wind speed in Canada

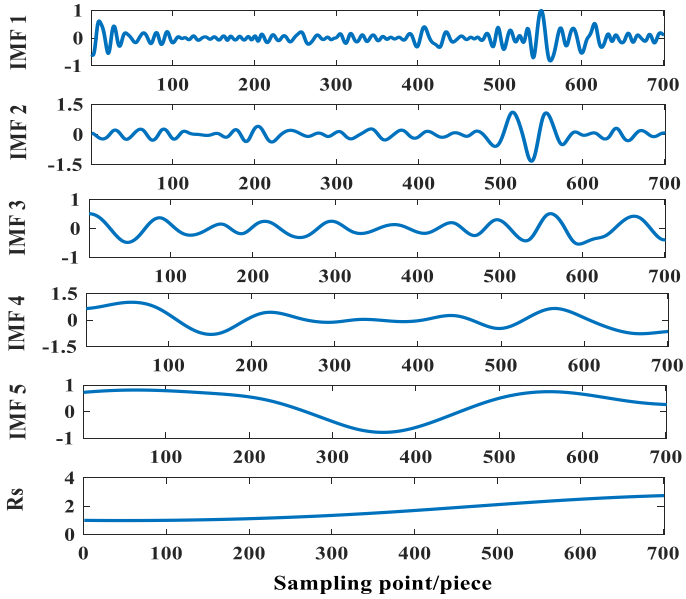

Fig.14 FEEMD effects of wind speed in Canada

In the above figure, EMD decomposes 7 IMFs and 1 Rs, EEMD decomposes 8 IMFs and 1 Rs, CEEMD decomposes 7 IMFs and 1 Rs, MEEMD decomposes 6 IMFs and 1 Rs, FEEMD only decomposes 5 IMFs and one Rs. This is because EMD, EEMD, and CEEMD directly decompose the original signal according to the frequency from high to low, while MEEMD and FEEMD first detect and eliminate abnormal wind speed signals, thereby reducing the number of components that are subsequently decomposed. This reduces the complexity of modeling on the one hand, and reduces the time spent on predictive modeling on the other hand. In addition, it can be seen from Figure 14 that after the FEEMD decomposition method starts from IMF_2, the frequency of the component changes from high to low, the component curve has a long period, and the trend is gradually flat.

Generally, the four indexes of completeness, orthogonality, number of components, and decomposition time are used to judge the advantages and disadvantages of decomposition results. The index of completeness (Index of Completeness, IC) refers to the root mean square error between the signal reconstructed by the decomposed IMFs and the remainder and the original signal. Orthogonality index (Index of Orthogonality, IO) refers to the orthogonal relationship between sub-sequences, and the size of IO can reflect the degree of modal aliasing. This paper

uses Index of overall Orthogonality (IOO), that is, the IO values of the decomposed components and the original signal to characterize the degree of modal aliasing of each decomposition method. The larger the IOO value, the more serious the degree of modal aliasing. The formulas of IC, IO, IOO are as follows:

$$C = \sqrt{\frac{\sum_{t=0}^{T}[x(t) - \sum_{i=1}^{N} c_i(t)]^2}{T}} \tag{13}$$

$$IO_{i,k} = \sum_{t=0}^{z} \frac{c_i(t)c_k(t)}{c_i(t) + c_k(t)} \tag{14}$$

$$IOO = \frac{1}{A(A-1)} \sum_{i,k=0}^{A} IO_{i,k}, i \neq k \tag{15}$$

In the formula, $x(t)$ is the original wind speed sequence, A is the number of components, T is the number of sampling points, and $c(t)$ is the decomposed component. The indicators for evaluating the five decomposition methods in Canada are shown in Table 1.

Tab.1 Decomposition evaluation indexes of five methods in Canada

Decomposition method	IOO	IC(m/s)	Number of components/piece	Time/s
EMD	0.2205	8.872	8	3.996
EEMD	0.1425	5.821	9	8.274
CEEMD	0.1386	5.581	8	6.347
MEEMD	0.1161	3.298	7	6.558
FEEMD	**0.0642**	**1.452**	**6**	**4.183**

It can be obtained from Table 1: From the perspective of IOO, the FEEMD is the lowest, indicating that compared with the other four methods, the degree of modal aliasing is the lightest after FEEMD decomposition; from the perspective of the completeness index (IC), it shows that the FEEMD decomposition method is more important. The structural error is the smallest; the number of components of the FEEMD method is 6, which is the smallest of the five decomposition methods; compared with the running time, the FEEMD decomposition method is not as short as the EMD method, but it is still within an acceptable range. The above indicators show that the FEEMD decomposition method is effective.

5.3 Modal merger of wind speed data in Canada

The PE value line chart of the FEEMD component in Canadian wind farm is shown in Figure 15.

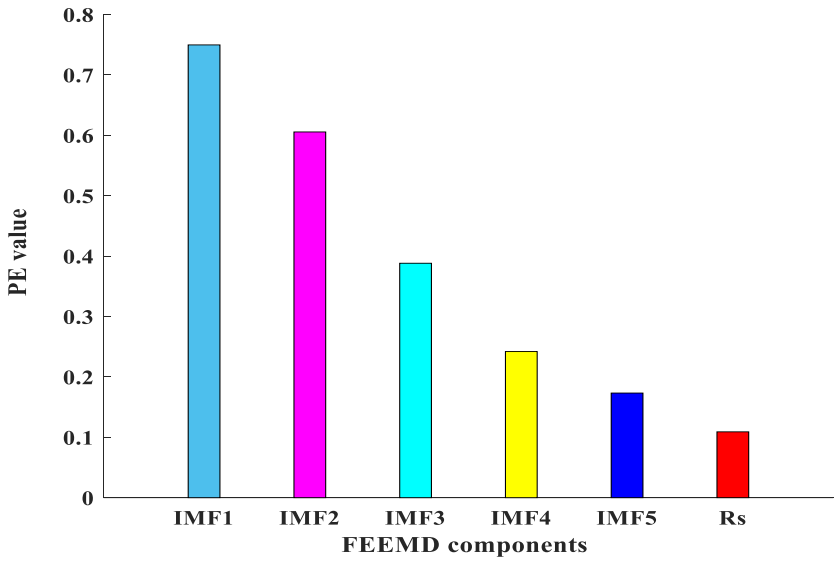

Fig.15 Sample entropy line graph of each IMF of FEEMD in Canadian wind farm

Table 2 shows the component results after modal merging in Canadian wind farm .

Tab. 2 New numbers with merged IMF component of FEEMD in Canadian wind farm

Original IMF component number	New serial number
1,2	1
3	2
4，5，6	3

5.4 Comparison experiment

To examine the superiority of the method proposed in this article, this article compares it with the eight models of WNN, ELM, BP, SSA-BP, EMD-SSA-BP, EEMD-SSA-BP, CEEMD-SSA-BP, MEEMD-SSA-BP. For describing the prediction effect of the proposed model(Wei Cao 2019; Xiujuan Tian et al. 2019), this paper uses five classic evaluation indexes to evaluate the experimental results, including Mean Absolute Error (MAE), Root Mean Square Error (RMSE), Error Sum of Squares (SSE) ,Mean Absolute Percentage Error (MAPE)and the goodness-of-fit (R^2).

$$MAE = \frac{1}{N}\sum_{n=1}^{N}\left|y_n - \hat{y}_n\right| \tag{16}$$

$$RMSE = \sqrt{\frac{1}{N}\sum_{n=1}^{N}(y_n - \hat{y}_n)^2} \tag{17}$$

$$SSE = \sum_{n=1}^{N}(y_n - \hat{y}_n)^2 \tag{18}$$

$$MAPE = \frac{1}{N}\sum_{n=1}^{N}\left|\frac{y_n - \hat{y}_n}{y_n}\right| \times 100\% \tag{19}$$

$$R^2 = \frac{\sum_{n=1}^{N}(\hat{y}_n - \bar{y})^2}{\sum_{n=1}^{N}(y_n - \bar{y})^2} \tag{20}$$

Which N represents the number of sample points, y_n refers to the actual value of the wind speed, $\hat{y}_n$ represents the prediction value of the wind speed, and $\bar{y}$ refers to the average value of the points.

5.4.1 Comparison of FEEMD with other decomposition methods

FEEMD overcomes modal aliasing in traditional decomposition, making decomposition results better.Therefore,we use FEEMD-SSA-BP model and EMD-SSA-BP, EEMD-SSA-BP, CEEMD-SSA-BP, MEEMD-SSA-BP model to predict the trend of wind speed time series. At the same time, to show that the prediction efficiency can be enhanced after the decomposition of the wind speed series in advance, we also introduced the SSA-BP model as a reference for comparison(Liang Tao 2021; Yagang Zhang et al. 2020). Figures 16-19 shows the comparison of the MAE, RMSE, MAPE, and SSE values of the six models of two wind farms. The dark blue bar, orange rectangular bar, yellow bar, purple bar, green bar and sky blue bar refer to the error value of SSA-BP、EMD-SSA-BP EEMD-SSA-BP、CEEMD-SSA-BP 、MEEMD-SSA-BP、FEEMD-PE-SSA-BP model respectively. From Figures 16-19, it can be deduceded that among the six models, the RMSE, MAE, MAPE, and SSE values of SSA-BP are the largest, while FEEMD-PE-SSA-BP model has the lowest error index values. It can be explained that: 1) The prediction result after the decomposition algorithm is used in advance for the wind speed time series is more accurate than the result of direct prediction. 2) Compared with EMD, EEMD, CEEMD, MEEMD, using FEEMD method to decompose the original wind speed series can get more accurate prediction results.

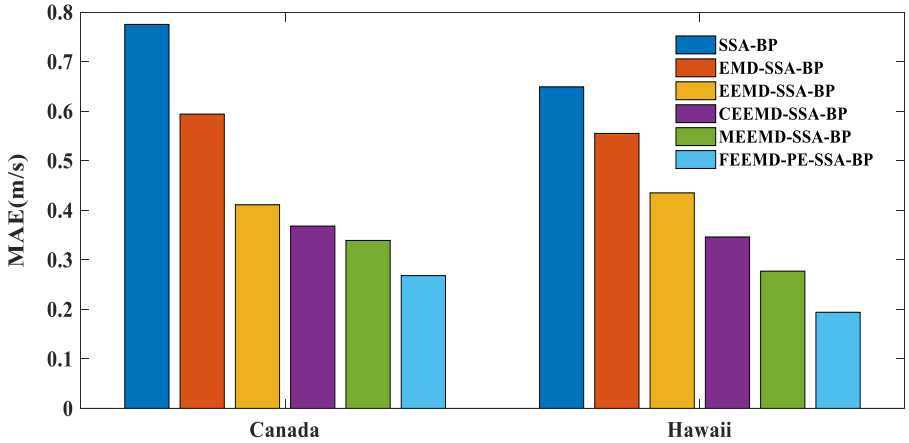

Fig.16 Comparison results of MAE values of six models of two wind farms

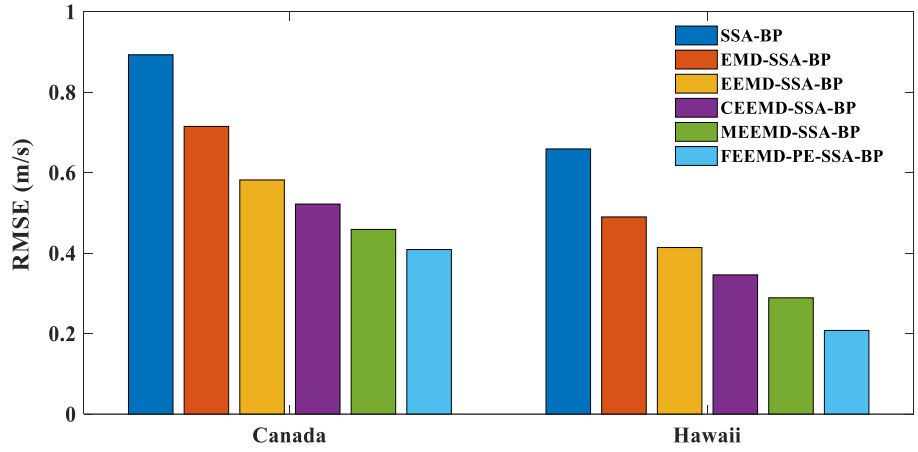

435

436 **Fig.17** Comparison results of RMSE values of six models of two wind farms

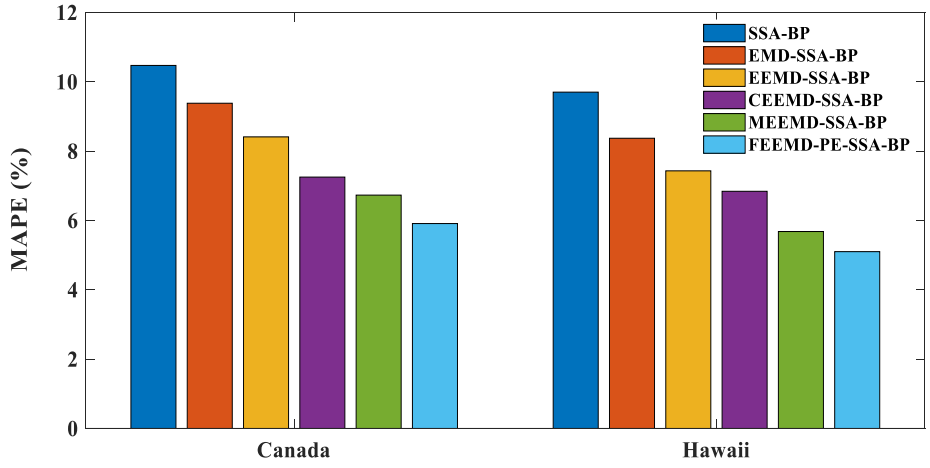

437

438 **Fig.18** Comparison results of MAPE values of six models of two wind farms

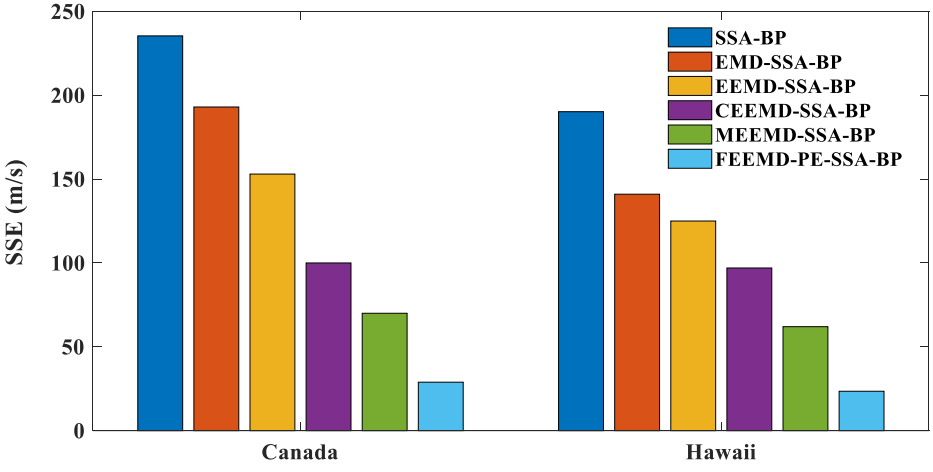

439

440 **Fig.19** Comparison results of SSE values of six models of two wind farms

441

442 ### 5.4.2 Comparison of BP and SSA-BP

443 Initial connection weight and threshold of BP neural network have a greater impact on network .
444 While it's hard to acquire the two parameters accurately, which leads to low model prediction
445 accuracy. To deal with the problem, sparrow search algorithm is introduced to optimize BP

network. It has a good global search performance, so that a better initial weight and threshold can be obtained. For the purpose of verifying the optimization effect of the sparrow search algorithm, The prediction errors of BP and SSA-BP are obtained in Figures 20-26. Figure 20-23 is a comparison of four error evaluation indexes of the two. The blue bar and the red bar show the error value of BP and SSA-BP respectively. It can be seen that the RMSE, MAE, MAPE, and SSE values of the prediction results obtained by SSA-BP model are obviously lower than only using BP. It can be concluded from Figure 24 that the SSA-BP models of the two wind farms have a higher degree of fit than the BP model. Figure 25-26 presents the prediction error curves of BP and SSA-BP. The green curve shows the prediction error of BP model, while the magenta curve means the error of SSA-BP. It can be obviously seen that the value of the green curve is closer to zero than magenta curve, which indicates SSA-BP model has higher prediction accuracy than BP. As a result, the initial weight and threshold value of BP network searched by sparrow search algorithm can receive better prediction results.

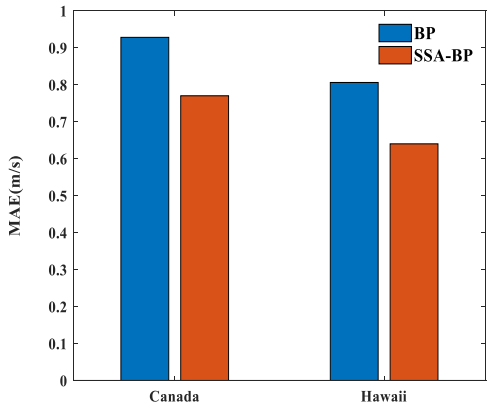

Fig.20 The MAE of BP and SSA-BP

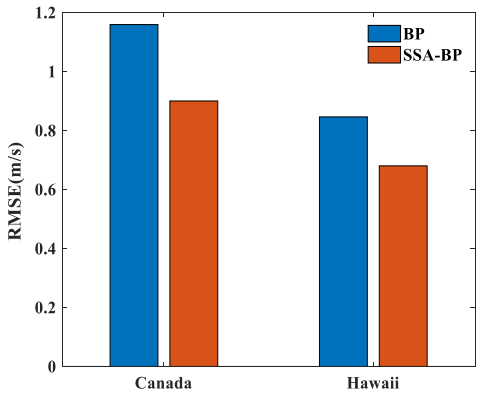

Fig.21 The RMSE of BP and SSA-BP

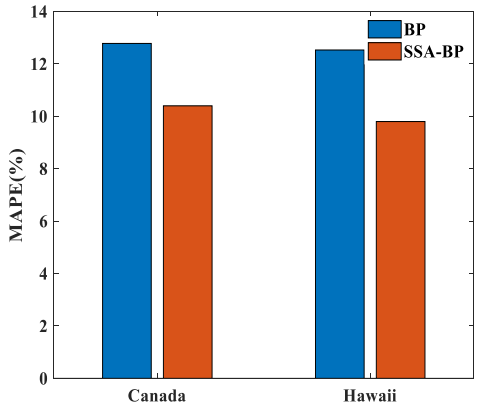

Fig.22 The MAPE of BP and SSA-BP

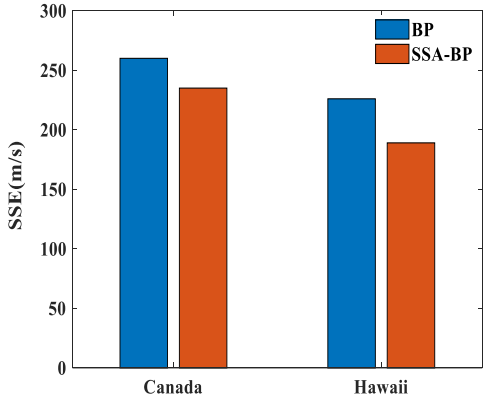

Fig.23 The SSE of BP and SSA-BP

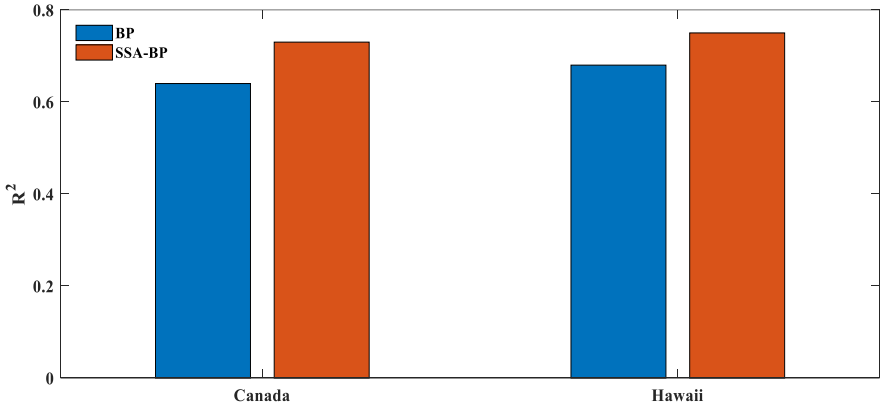

463

464 **Fig.24** The R^2 of BP and SSA-BP

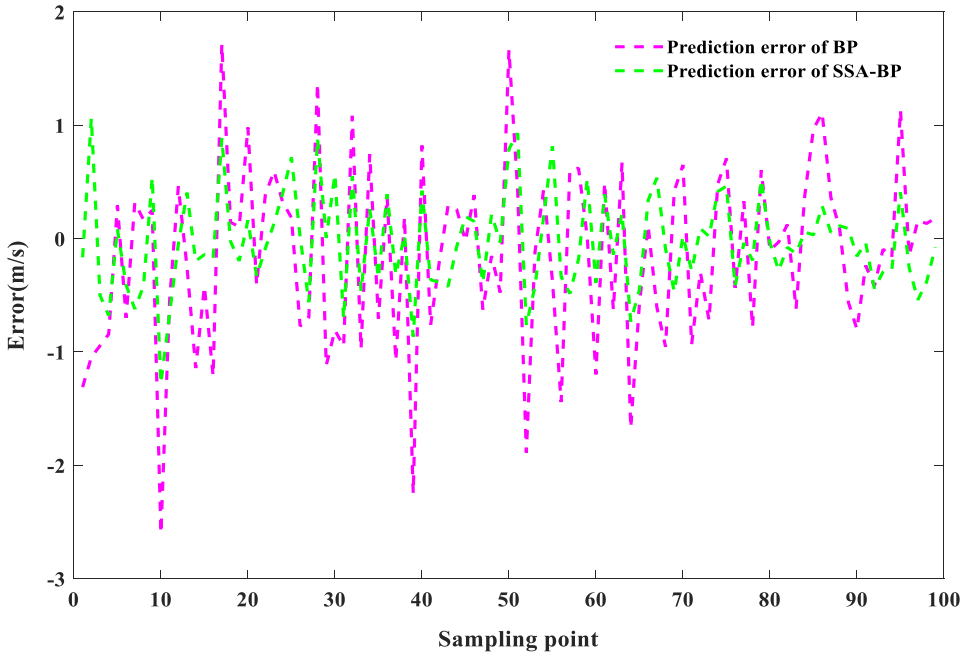

465

466 **Fig.25** The comparison of BP and SSA-BP of **Canada**

467

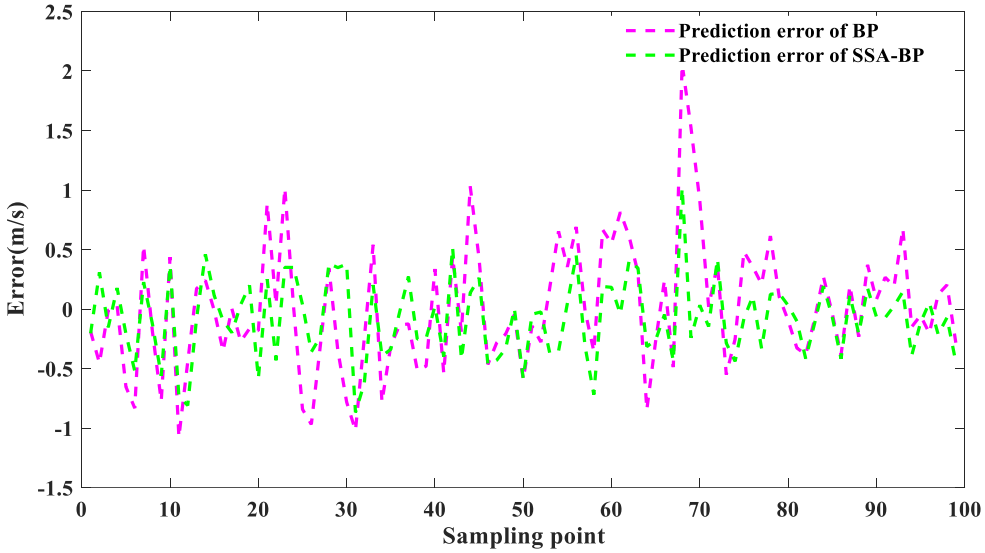

Fig.26 The comparison of BP and SSA-BP of **Hawaii**

5.4.3.Comparison of other traditional neural network model and FEEMD-PE-SSA-BP model

In the part, WNN 、BP、 ELM model and FEEMD-PE-SSA-BP model were used to examine the wind speed data of two wind farms. The prediction results of the four models are presented in Figure 27-28. The red curve is the real wind speed time series, while the blue dashed curve shows the trend of WNN, and magenta dashed curve means the forecasting result of ELM. The purple dotted line represents the forecasting result of BP, while the yellow dotted line shows the result of FEEMD-PE-SSA-BP model. It can be obviously seen that only the trend of blue curve differs greatly from the true value, which indicates that the result of WNN is the worst. Besides, the trend of the purple curve and magenta curve are relatively close, but in some places, the fitting effect of the red curve is not good, which shows that BP and ELM model can predict the basic trend of wind speed, but the forecasting accuracy isn't very high. The trend of red curve and yellow curve in the figure are basically the same, indicating that the prediction result of the model proposed in this paper is the closest to the true value, and the forecasting result is the best. As a result, compared with the traditional prediction models, the FEEMD-PE-SSA-BP model has better forecasting performance and is more suitable for wind speed prediction.

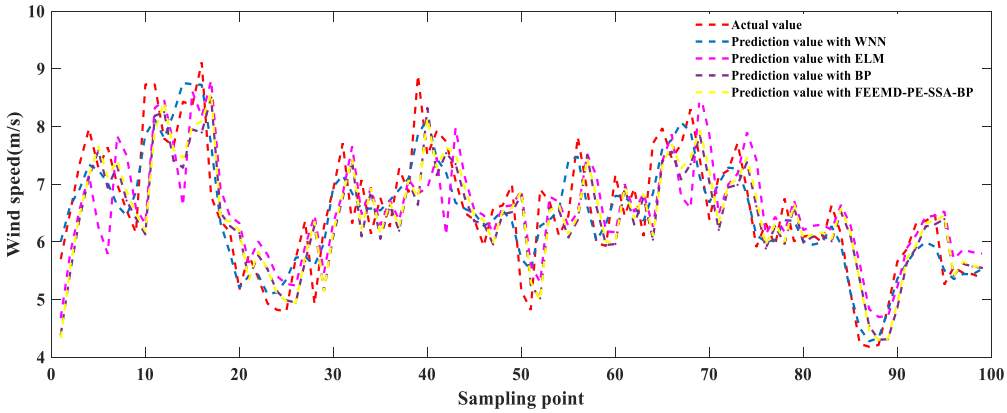

Fig.27 Comparison with traditional prediction model of **Canada**

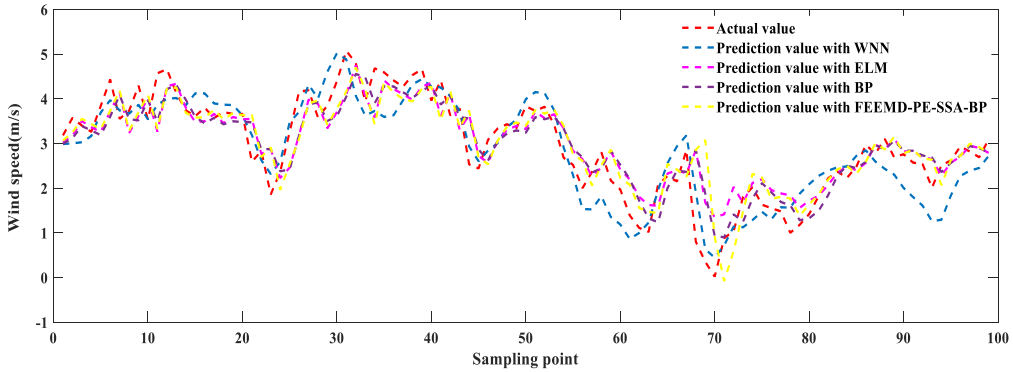

Fig.28 Comparison with traditional prediction model of **Hawaii**

So as to describe the prediction effects more accurately, the MAE, RMSE, MAPE, SSE and R^2 are calculated respectively. As shown in Table 3, the prediction error is much lower than the other three models, indicating that the prediction accuracy of FEEMD-PE-SSA-BP model is better than the traditional forecasting models.

Tab.3 Model error results

Wind Farm		**Canada**					**Hawaii**				
Evaluation Index		MAE (m/s)	RMSE (m/s)	MAPE (%)	SSE (m/s)	R^2	MAE (m/s)	RMSE (m/s)	MAPE (%)	SSE (m/s)	R^2
Model	WNN	1.414	1.232	17.15	288.3	0.439	0.953	0.903	16.35	259.6	0.499
	ELM	1.325	1.248	16.75	273.4	0.512	0.878	0.852	15.72	248.1	0.547
	BP	0.928	1.159	12.78	262.7	0.645	0.806	0.846	14.53	231.5	0.672
	FEEMD-PE-SSA-BP	**0.278**	**0.423**	**6.34**	**32.70**	**0.909**	**0.219**	**0.230**	**5.32**	**28.81**	**0.946**

6 Conclusion

The rapid development of the global economy and society has made the contradiction between the supply of primary energy sources such as oil and environmental protection increasingly prominent, and it has also accelerated the outbreak of the traditional energy crisis. As a kind of clean and environmentally friendly renewable energy, wind energy is more and more favored by countries all over the world. With the improvement of science and technology, the national energy strategy is increasingly adjusted to the direction of clean energy such as hydropower and wind energy. The proposal of the "three types, two networks, world-class" construction strategy will vigorously promote the high quality of our country's energy industry and sustainable development. With the continuous increase in the scale of wind power grid connection, the uncertainties and nonlinear characteristics of wind speed have put a lot of pressure on power system. The accurate forecasting of wind speed in advance is an important way to solve this problem, and it can be used for the operation of wind farms and automatic power generation control (AGC), which can provide necessary information to improve the ability of wind power bidding on the Internet.

Wind speed prediction for wind farms is beneficial to the operation of wind farms and flexible scheduling of power grids containing flexible scheduling of the grid with new energy sources, but

the wind speed is random and has low energy density, which will lead to the reliability of power system operation. The reliability of power system operation will be reduced. Therefore, accurate wind speed prediction is essential for wind power grid connection and power system operation. Therefore, accurate wind speed prediction becomes more and more important for grid-connected wind power and power system operation. Therefore, in this paper, first and foremost, FEEMD method is introduced to process original wind speed data to obtain multiple IMF components. Then combining the IMFs with similar sample entropy into NIMFs. After that, the sparrow search algorithm is introduced to promote the prediction results. In a nutshell, the model on one hand fully explores the law of wind speed changes by dealing with historical data, and on the other hand, it uses FEEMD to shape undulation components from different scales, which can significantly enhance the wind speed prediction accurancy, and then guarantee the development of renewable energy.

Through above comparative experiments, it can be verified that (1)FEEMD uses the box-counting dimension to eliminate the abnormal signals in the original signal and then decomposes the remaining signals. On the one hand, it can solve the problem of modal aliasing in EMD, and on the other hand, it can also avoid unnecessary integration averaging in the EEMD and CEEMD methods. It not only reduces the calculation amount of EEMD and CEEMD, but also reduces the reconstruction error, which guarantees the completeness of decomposition and obtains better decomposition results; (2) BP neural network is optmized by SSA, which can effectively improve the prediction accuracy of wind speed; (3)FEEMD-PE-SSA-BP model has higher prediction accuracy when compared with the traditional neural network prediction models.

Due to the inherent instability and volatility of wind speed data, there is currently no predictive model that can predict wind power perfectly. Scholars and researchers need to continue to explore and study.

Ethical Approval

Not applicable.

Consent to Participate

Not applicable.

Consent to Publish

Not applicable.

Authors Contributions

Zhu Ting: Conceptualization, Methodology, Software,Writing original draft.

Wenbo Wang: Model building;

Min Yu: Writing review&editing;

Funding

This work was supported in part by the National Natural Science Foundation of China under Grant 61671338 and Grant 51877161.

Competing Interests

The authors declare that they have no competing interests.

Availability of data and materials

The datasets that has been used in the study are available from co-author on reasonable request.

Author Information

Affiliations

School of Science, Wuhan University of Science and Technology, Wuhan 430081, China

Ting Zhu, Wenbo Wang & Min Yu

Corresponding author

Min Yu (zhuting20210422@163.com)

Acknowledgements

The authors thank the anonymous referees for the thoughtful and constructive suggestions that led to a considerable improvement of the paper.

References

Aasim,S.N. Singh,Abheejeet Mohapatra. Repeated wavelet transform based ARIMA model for very short-term wind speed forecasting[J]. Renewable Energy,2019,136:

Bo Ming,Pan Liu,Shenglian Guo,Lei Cheng,Jingwen Zhang. Hydropower reservoir reoperation to adapt to large-scale photovoltaic power generation[J]. Energy,2019,179:

Chen Gonggui,Tang Bangrui,Zeng Xianjun,Zhou Ping,Kang Peng,Long Hongyu. Short-term wind speed forecasting based on long short-term memory and improved BP neural network[J]. International Journal of Electrical Power and Energy Systems,2022,134:

Cui Yanbin,Huang Chenchen,Cui Yanping. A novel compound wind speed forecasting model based on the back propagation neural network optimized by bat algorithm.[J]. Environmental science and pollution research ,2020,27(7):

Fuzheng Liu,Junwei Gao,Huabo Liu. A Fault Diagnosis Solution of Rolling Bearing Based on MEEMD and QPSO-LSSVM[J]. IEEE Access,2020,8:

Gupta, D., Natarajan, N. & Berlin, M. Short-term wind speed prediction using hybrid machine learning techniques. Environmental science and pollution research (2021).

HHT endpoint effect suppression method based on double symmetry continuation[J]. Xiang Hong, Wu Chen, Du Xipeng. Journal of Fujian University of Technology. 2016(04).

Huang Norden E.,Shen Zheng,Long Steven R.,Wu Manli C.,Shih Hsing H.,Zheng Quanan,Yen Nai-Chyuan,Tung Chi Chao,Liu Henry H.. The empirical mode decomposition and the Hilbert spectrum for nonlinear and non-stationary time series analysis[J]. Proceedings of the Royal Society A: Mathematical, Physical and Engineering Sciences,1998,454(1971):

Huanling Hu,Lin Wang,Rui Tao. Wind speed forecasting based on variational mode decomposition and improved echo state network[J]. Renewable Energy,2021,164:

Hui Liu,Haiping Wu,Yanfei Li. Smart wind speed forecasting using EWT decomposition, GWO evolutionary optimization, RELM learning and IEWT reconstruction[J]. Energy Conversion and Management,2018,161:

Hui Liu,Zhu Duan,Feng-ze Han,Yan-fei Li. Big multi-step wind speed forecasting model based on secondary decomposition, ensemble method and error correction algorithm[J]. Energy Conversion and Management,2018,156:

Jaseena K.U.,Kovoor Binsu C.. Decomposition-based hybrid wind speed forecasting model using deep bidirectional LSTM networks[J]. Energy Conversion and Management,2021,234:

Jiankai Xue . Research and application of a new type of swarm intelligence optimization technology [D]. Donghua University, 2020.

Jinde Zheng, Junsheng Cheng, Yu Yang. Partly ensemble empirical mode decomposition: An improved noise-assisted method for eliminating mode mixing[J]. Signal Processing, 2014, 96.

Jinde Zheng, Junsheng Cheng, YuYang. Improved EEMD algorithm and its application research[J]. Vibration and Shock, 2013, 32(21): 21-26+46.

K U Jaseena,Kovoor Binsu C. A Wavelet-based hybrid multi-step Wind Speed Forecasting model using LSTM and SVR[J]. Wind Engineering,2021,45(5):

Li Dan,Jiang Fuxin,Chen Min,Qian Tao. Multi-step-ahead wind speed forecasting based on a hybrid decomposition method and temporal convolutional networks[J]. Energy,2022,238(PC):

Liang Tao,Zhao Qing,Lv Qingzhao,Sun Hexu. A novel wind speed prediction strategy based on Bi-LSTM, MOOFADA and transfer learning for centralized control centers[J]. Energy,2021,230:

Liang Tao,Zhao Qing,Lv Qingzhao,Sun Hexu. A novel wind speed prediction strategy based on Bi-LSTM, MOOFADA and transfer learning for centralized control centers[J]. Energy,2021,230:

Liao Xuechao,Liu Zhenxing,Deng Wanxiong. Short-term wind speed multistep combined forecasting model based on two-stage decomposition and LSTM[J]. Wind Energy,2021,24(9):

Qin Zhou, Pengjian Shang, Weighted multiscale cumulative residual Rényi permutation entropy of financial time series, Physica A: Statistical Mechanics and its Applications,2020,540,123089

Renato Huzak, Vlatko Crnković, Domagoj Vlah, Fractal dimensions and two-dimensional slow-fast systems, Journal of Mathematical Analysis and Applications,2021,501,2,125212.

Shouxiang Wang,Na Zhang,Lei Wu,Yamin Wang. Wind speed forecasting based on the hybrid ensemble empirical mode decomposition and GA-BP neural network method[J]. Renewable Energy,2016,94:

Terrien J,Marque C,Karlsson B.Automatic detection of mode mixing in empirical mode decomposition using nonstationarity detection:application to selecting IMFs of interest and denoising[J].EURASIP Journal on Advances in Signal Processing 2011,2011:37.

The closest similar distance continuation method and the parallel continuation method to suppress the end effect of EMD[J]. He Zhenpeng,Zhu Zhiqi,Xie Haichao,Wang Yawen,Li Zongqiang,He Rui,Du Chaoping,Li Jinlan. Mechanical Science and Technology. 2018(07).

Tian X, Yu D, Xing X, Wang S, Wang Z. Hybrid short-term traffic flow prediction model of intersections based on improved complete ensemble empirical mode decomposition with adaptive noise. Advances in Mechanical Engineering. April 2019.

Treatment of EMD Endpoint Problem Based on Polynomial Fitting Algorithm[J]. Liu Huiting, Zhang Min, Cheng Jiaxing. Computer Engineering and Applications. 2004(16).

Using mirror continuation and RBF neural network to deal with the end effect in EMD[J]. Han Jianping, Qian Jiong, Dong Xiaojun. Vibration. Testing and Diagnosis. 2010(04).

Wei Cao , Changliang Liu, Ziqi Wang, Haijun Li. Research on ultra-short-term prediction of wind power based on MEEMD and permutation entropy[J]. Renewable Energy, 2019, 37(03): 439-444

Wenlong Fu,Kai Wang,Chaoshun Li,Jiawen Tan. Multi-step short-term wind speed forecasting approach based on multi-scale dominant ingredient chaotic analysis, improved hybrid GWO-SCA optimization and ELM[J]. Energy Conversion and Management,2019,187:

Wu Z H,Huang N E.Ensemble empirical mode decomposition: A noise assisted data analysis method[J].Advances in Adaptive Data A-nalysis,2009,1:1-41.

Xiao J,Borgnat P,Flandrin P.Testing stationary with time frequency surrogates[J].in XVth European Signal Procedings Conference,Poznan,Poland,2007:2020-2040.

Xiujuan Tian,Dexin Yu,Xue Xing,Shiguang Wang,Zhuorui Wang. Hybrid short-term traffic flow prediction model of intersections based on improved complete ensemble empirical mode decomposition with adaptive noise[J]. Advances in Mechanical Engineering,2019,11(4):

Yagang Zhang,Guifang Pan,Bing Chen,Jingyi Han,Yuan Zhao,Chenhong Zhang. Short-term wind speed prediction model based on GA-ANN improved by VMD[J]. Renewable Energy,2020,156.

Yanfei Li,Haiping Wu,Hui Liu. Multi-step wind speed forecasting using EWT decomposition, LSTM principal computing, RELM subordinate computing and IEWT reconstruction[J]. Energy Conversion and Management,2018,167:

Yeh J R, Shieh J S. Complementary ensemble empirical mode decomposition: W u Z H, Huang N E. Ensemble empirical mode decomposition: A noise assisted data analysis method [J]. Advances in Adaptive Data Analysis, 2010, 2(2): 135-156.

723 Zhang Shuai,Chen Yong,Xiao Jiuhong,Zhang Wenyu,Feng Ruijun. Hybrid wind speed forecasting model based on
724 multivariate data secondary decomposition approach and deep learning algorithm with attention mechanism[J].
725 Renewable Energy,2021,174:
726 Zhou Shenghang,Xie Hao,Zhang Chuncheng,Hua Yingzi,Zhang Wenhui,Chen Qian,Gu Guohua,Sui Xiubao.
727 Wavefront-shaping focusing based on a modified sparrow search algorithm[J]. Optik,2021,244: